Nucleophilic Ring-opening of *meso*-Substituted 5-Oxaporphyrin

by Oxygen, Nitrogen, Sulfur, and Carbon Nucleophiles

Kazuhisa Kakeya, Masakatsu Aozasa, Tadashi Mizutani,* Yutaka Hitomi and Masahito Kodera

Department of Molecular Chemistry and Biochemistry, Faculty of Science and Engineering, and Center for Nanoscience Research, Doshisha University, Kyotanabe, Kyoto 610-0321, Japan

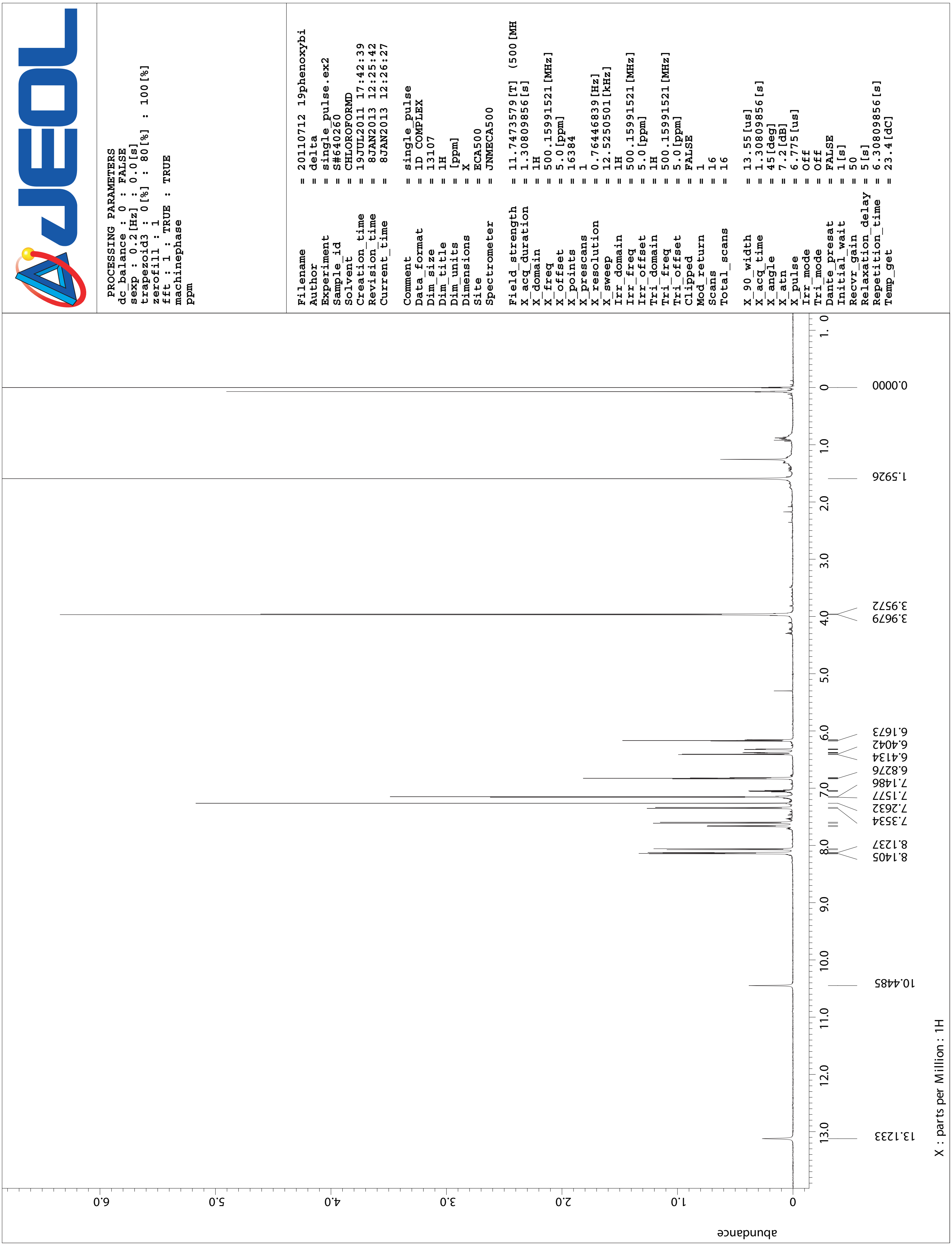

Figure S1. ^{1}H NMR of **4**.

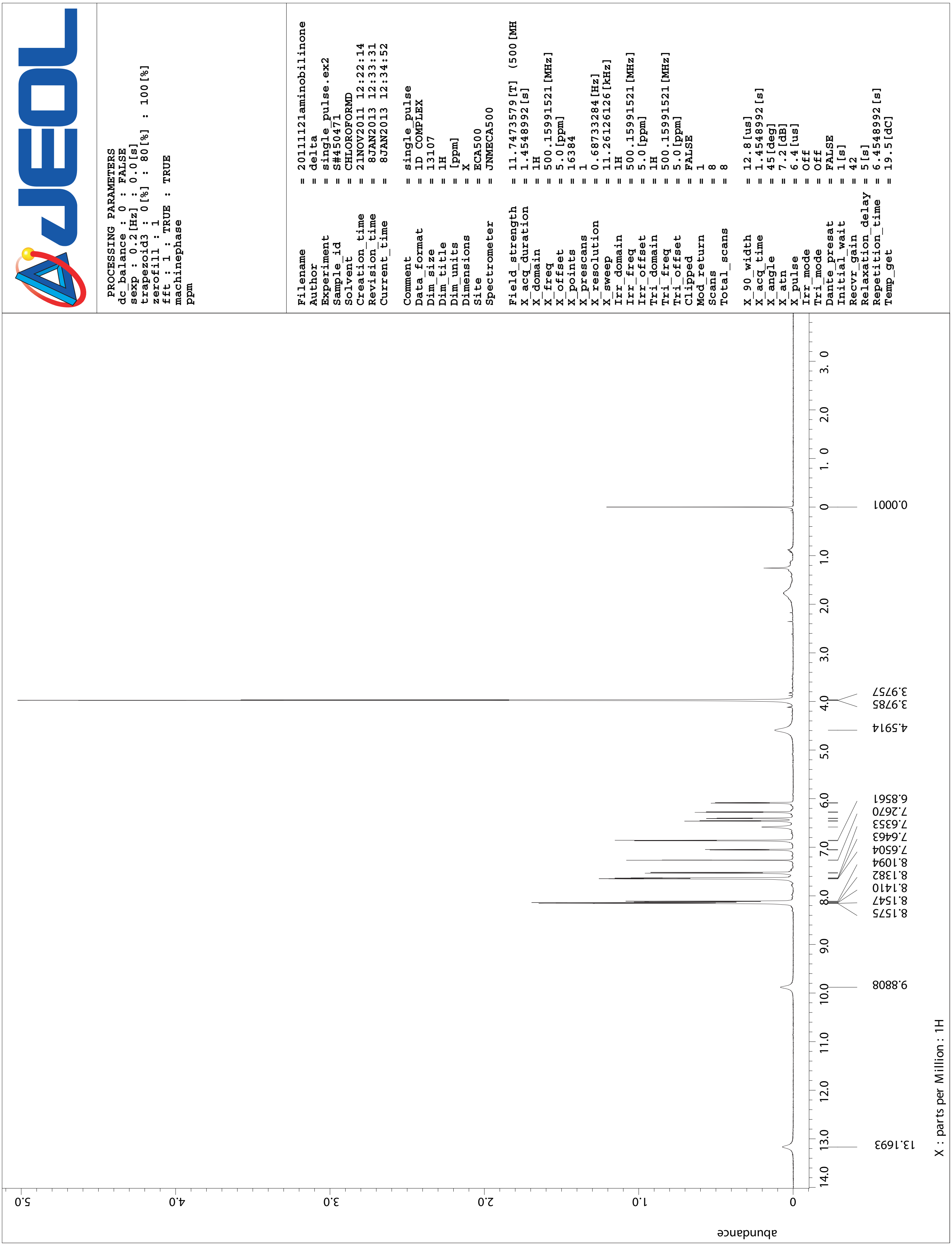

Figure S2. [1]H NMR of **5**.

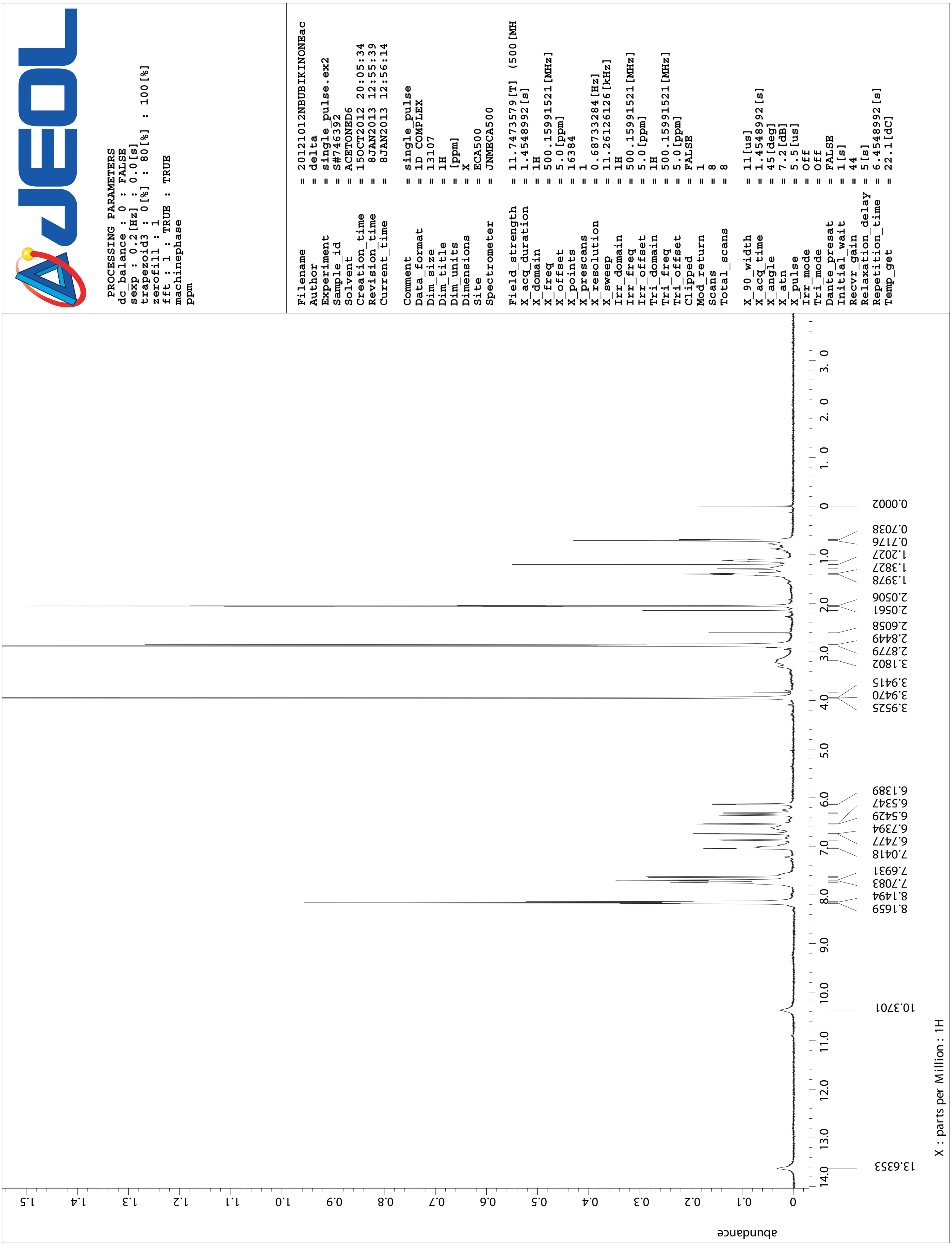

Figure S3. [1]H NMR of **6**.

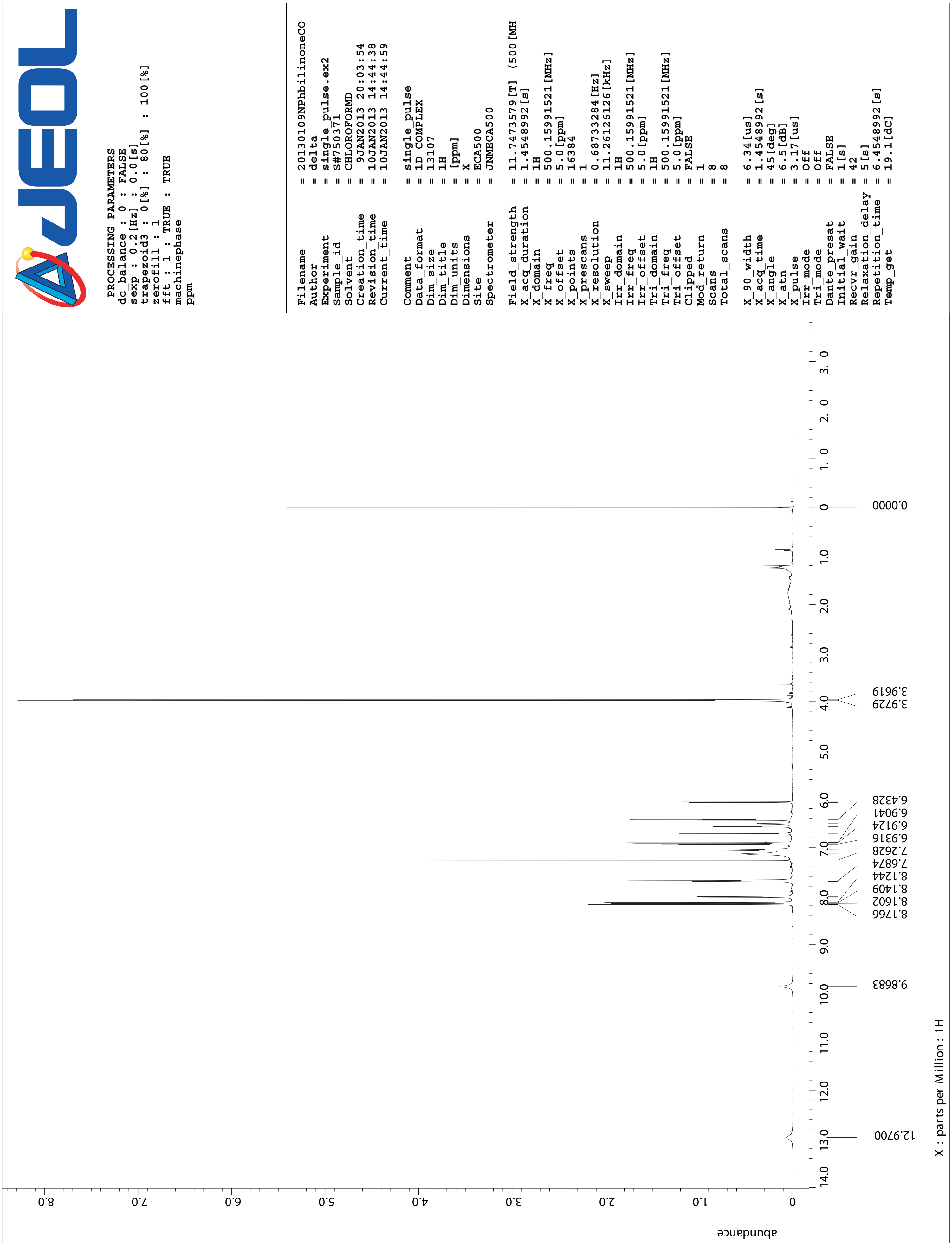

Figure S4. ^{1}H NMR of **7**.

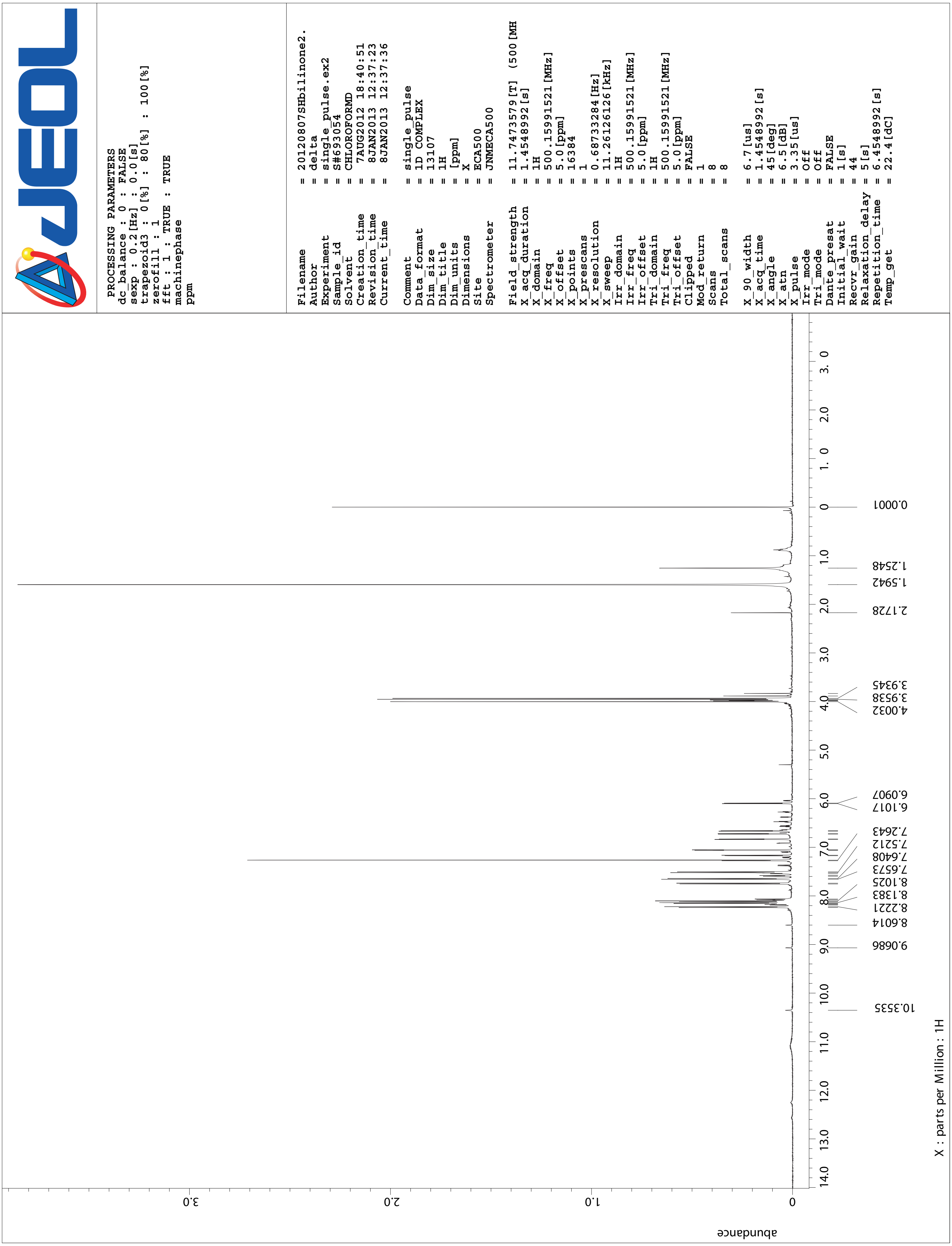

Figure S5. ^{1}H NMR of **8**.

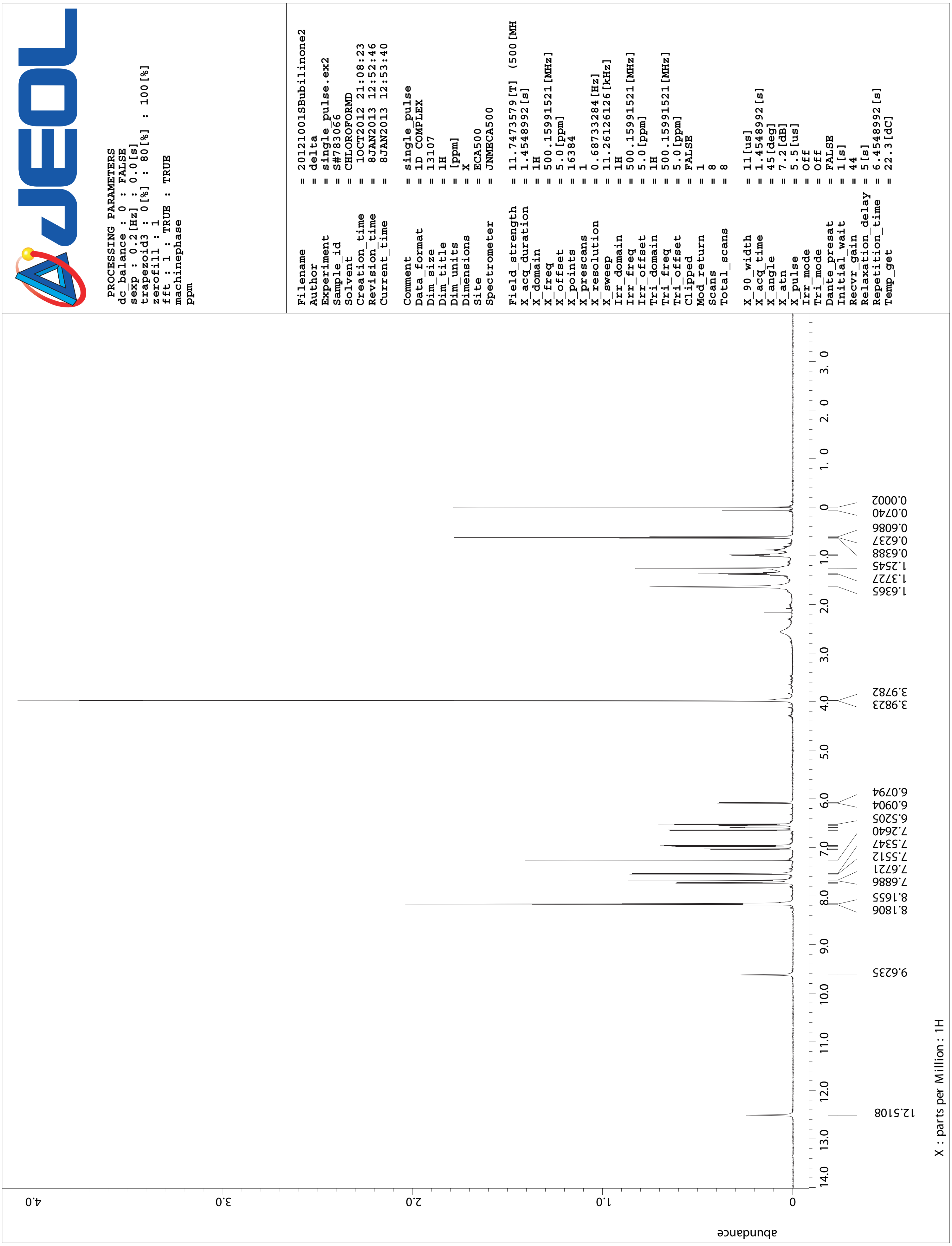

Figure S6. [1]H NMR of **9**.

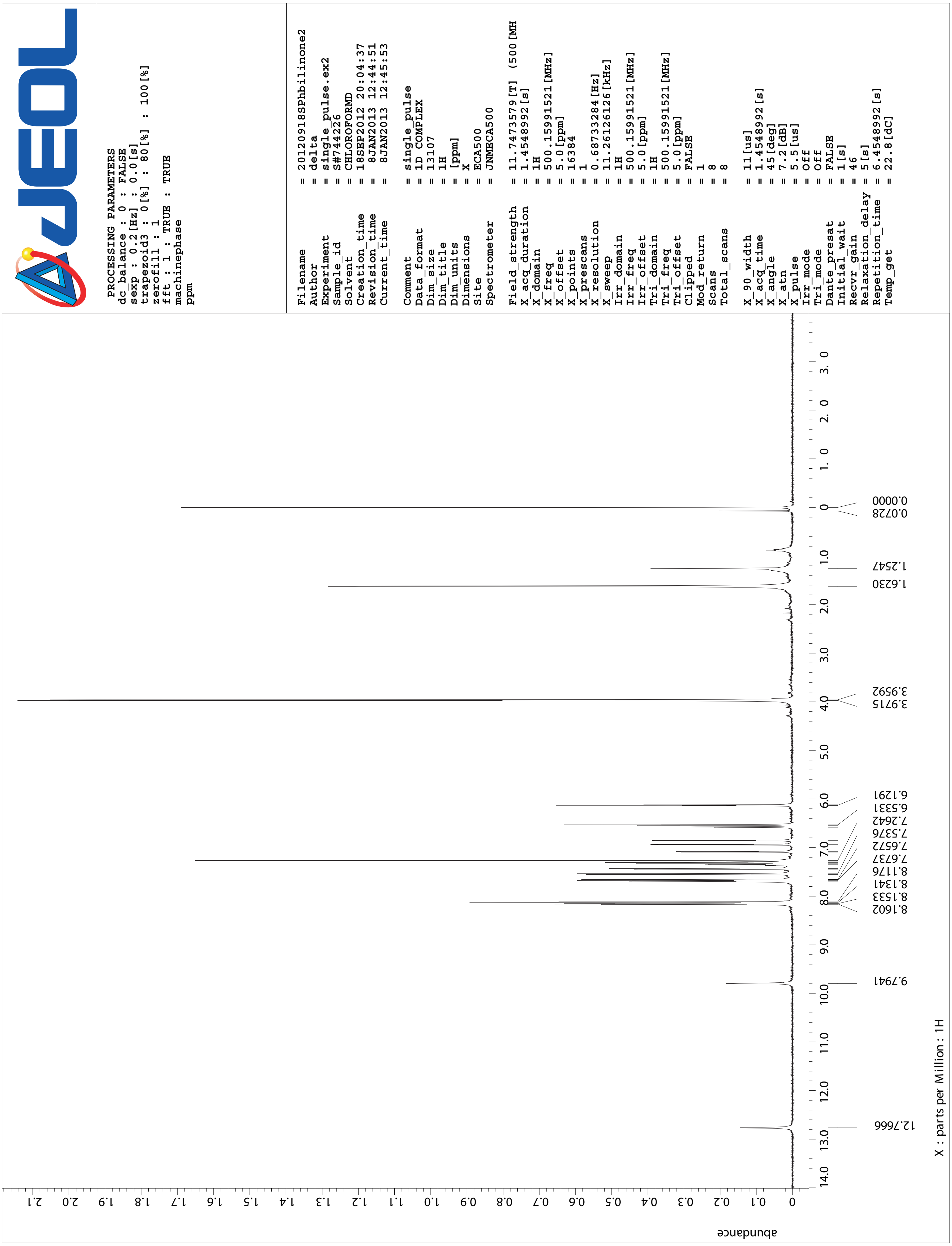

Figure S7. ^{1}H NMR of **10**.

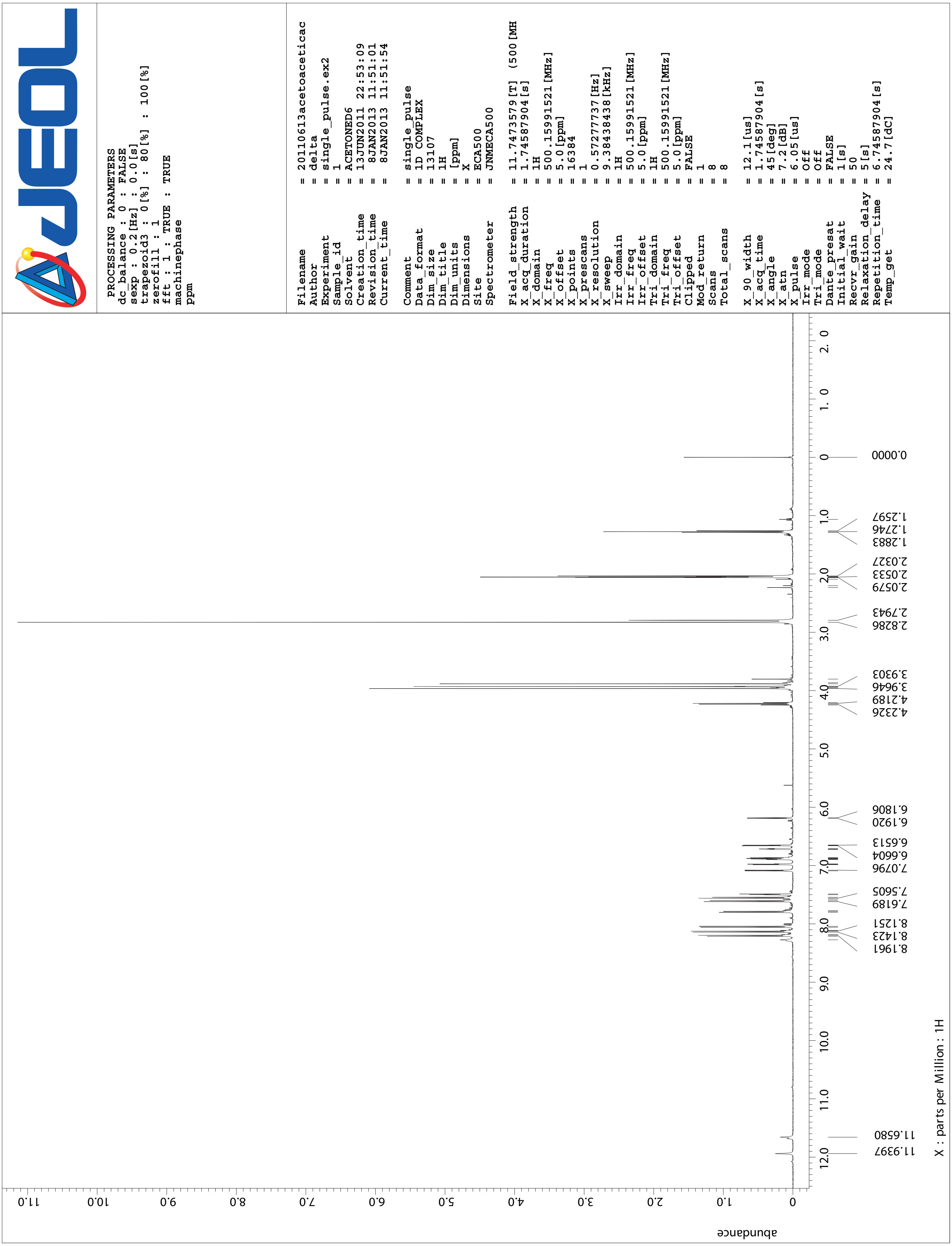

Figure S8. [1]H NMR of **11**.

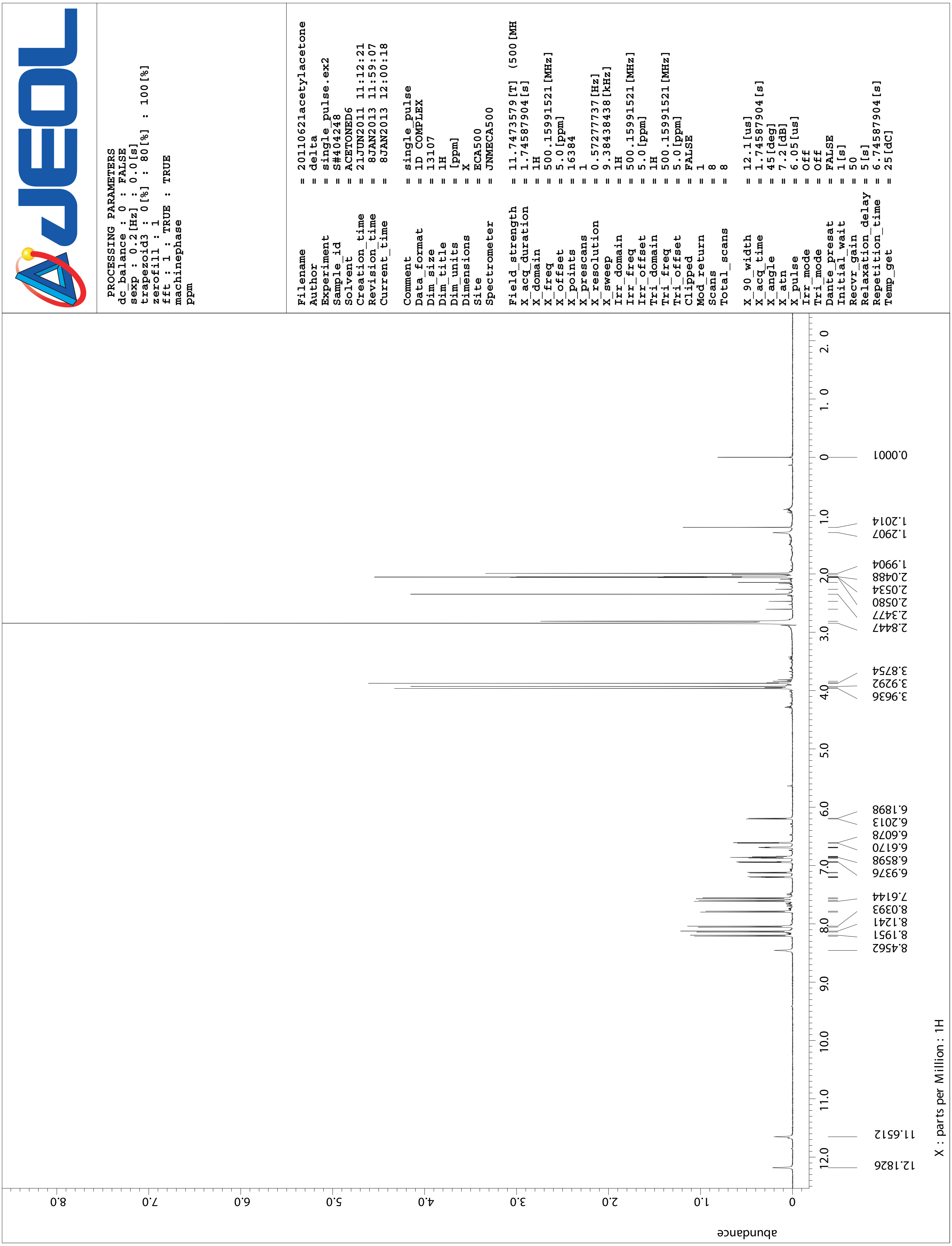

Figure S9. ^{1}H NMR of **12**.

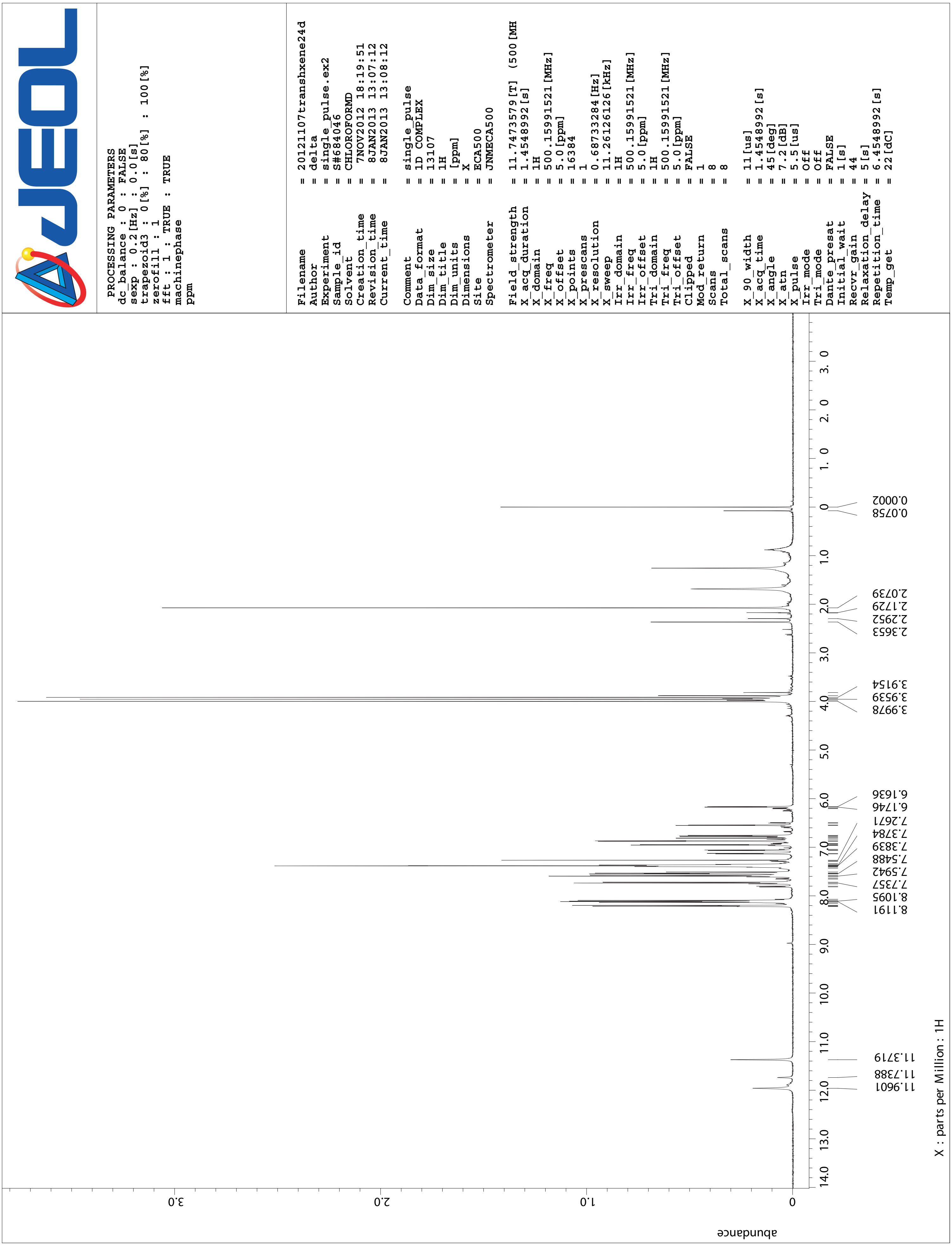

Figure S10. ^{1}H NMR of **13**.

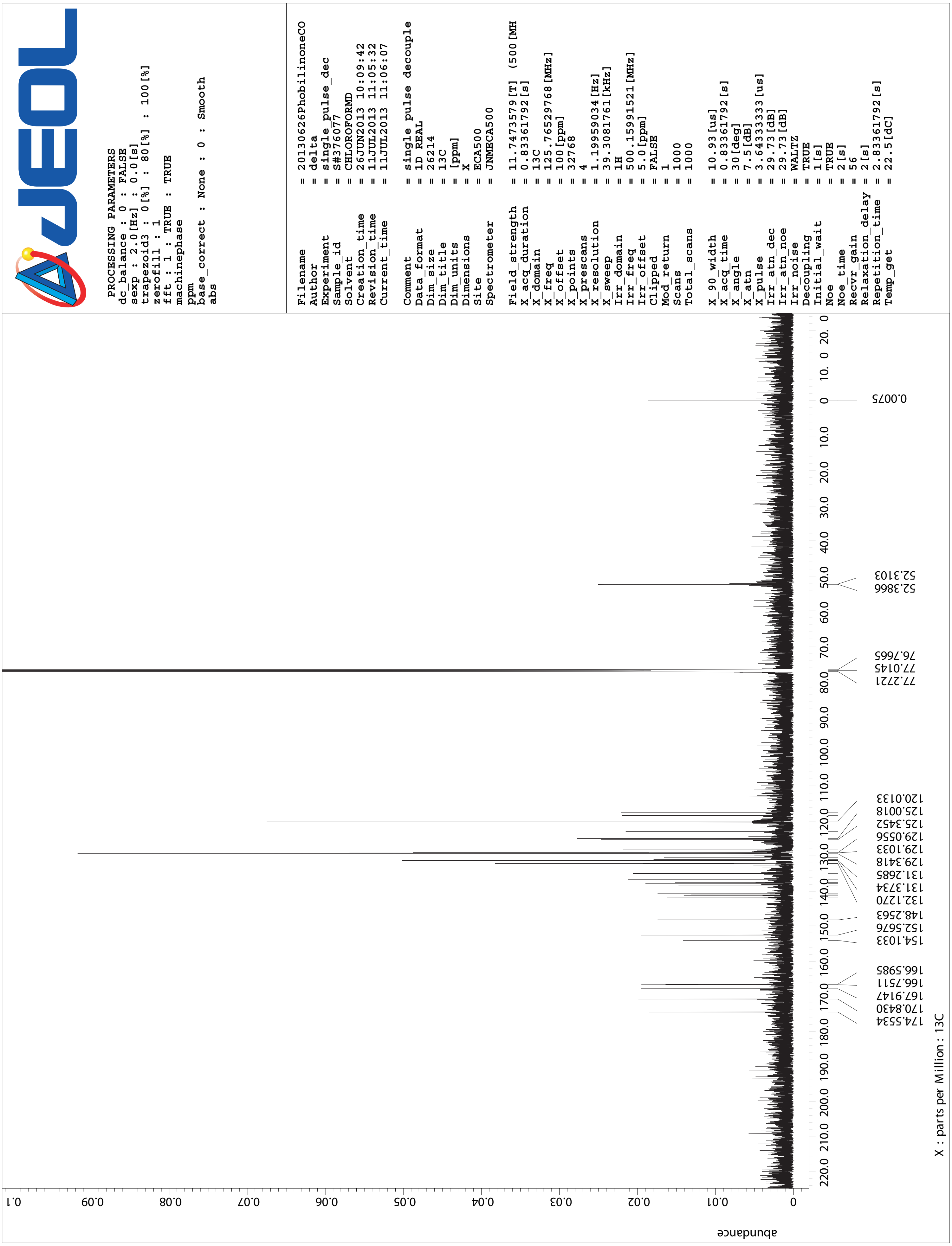

Figure S11. ^{13}C NMR of **4**.

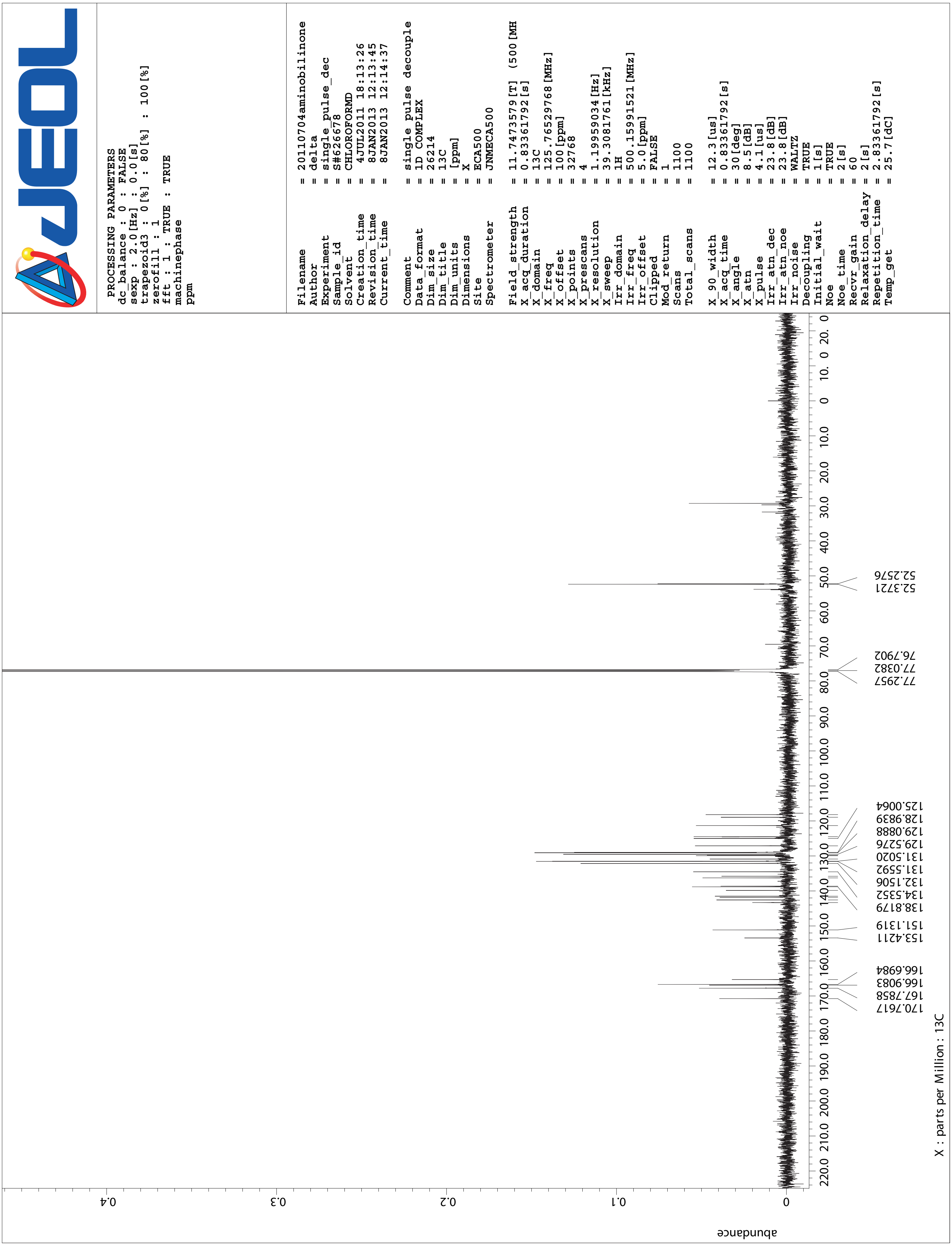

Figure S12. ^{13}C NMR of **5**.

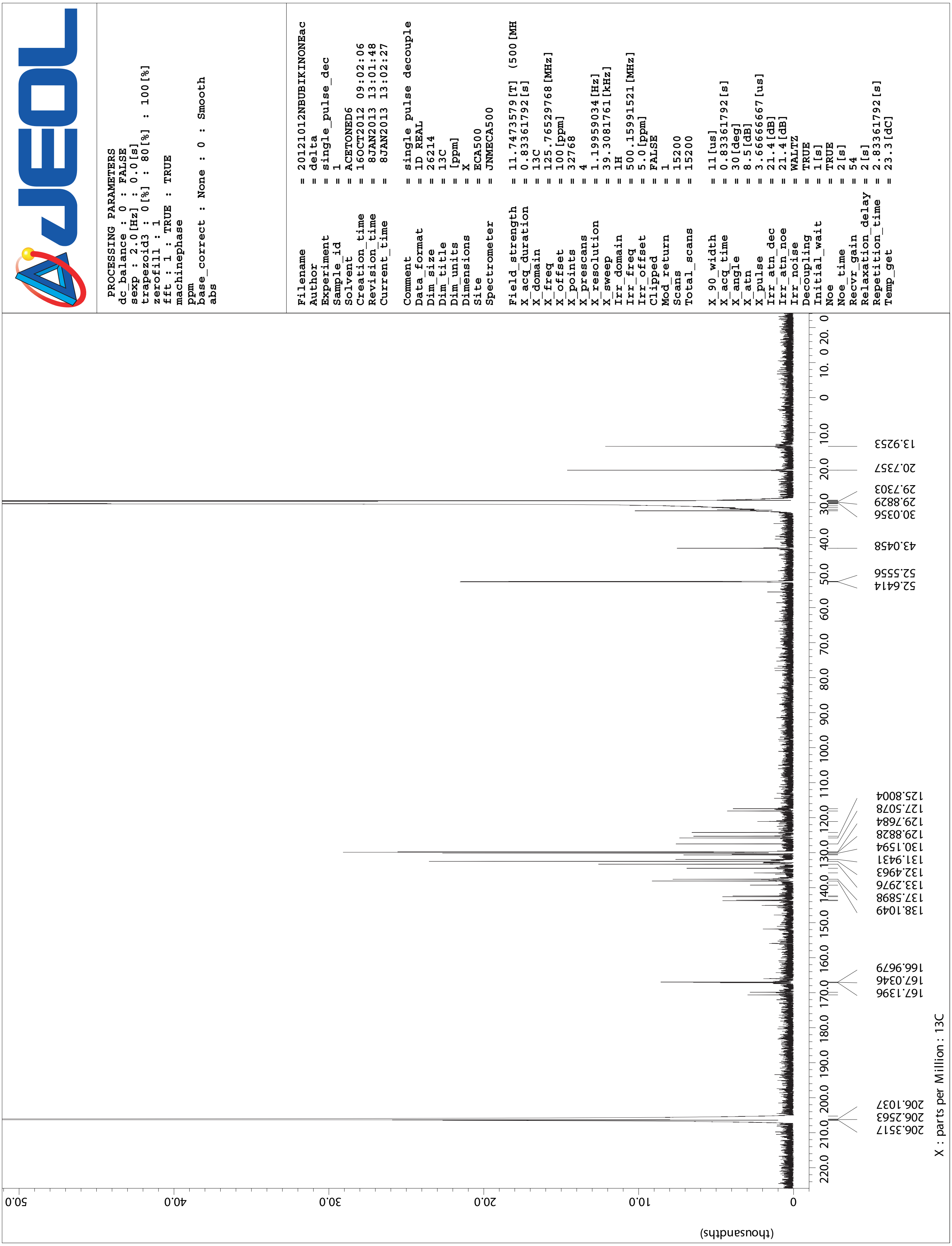

Figure S13. ^{13}C NMR of **6**.

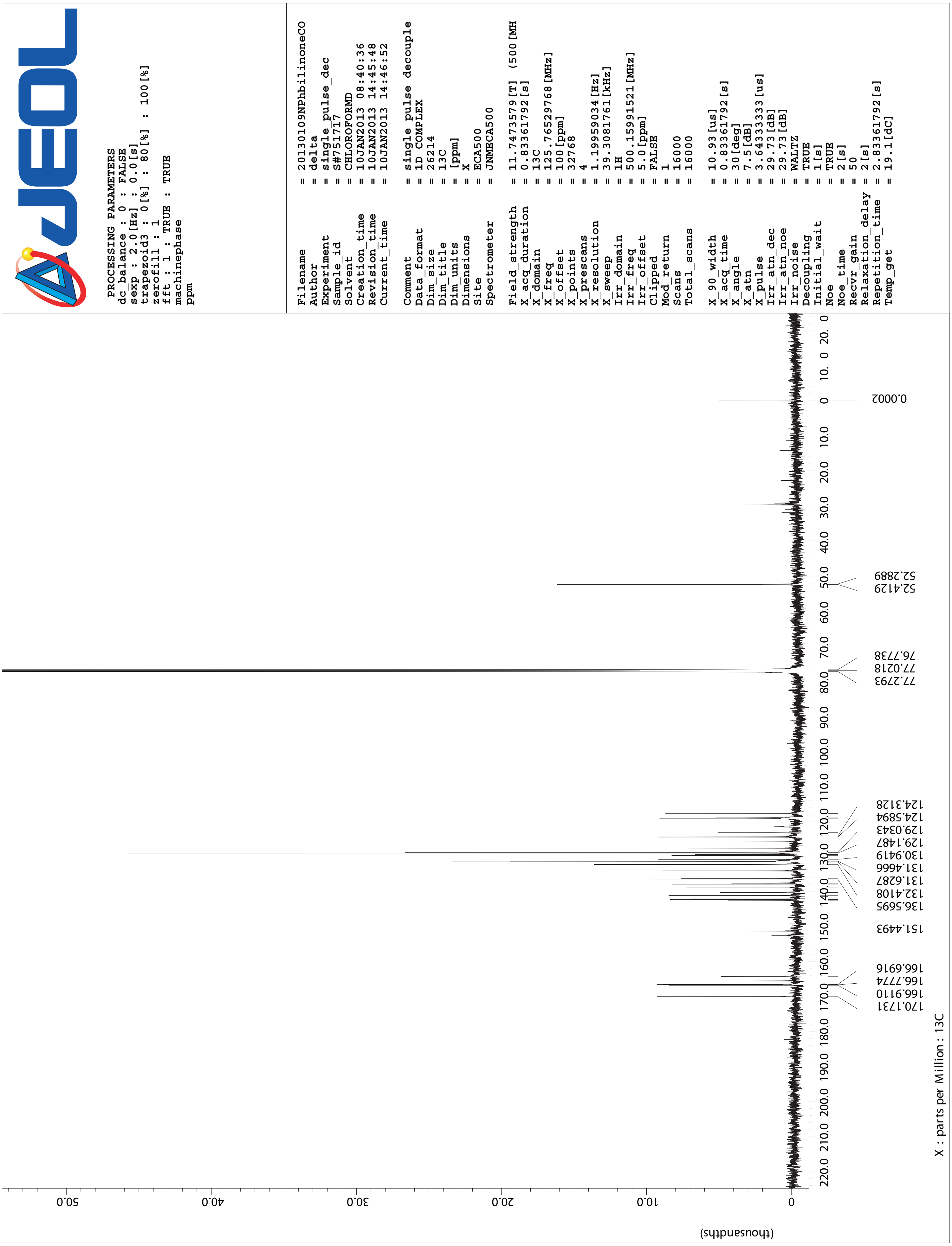

Figure S14. [1]H NMR of **7**.

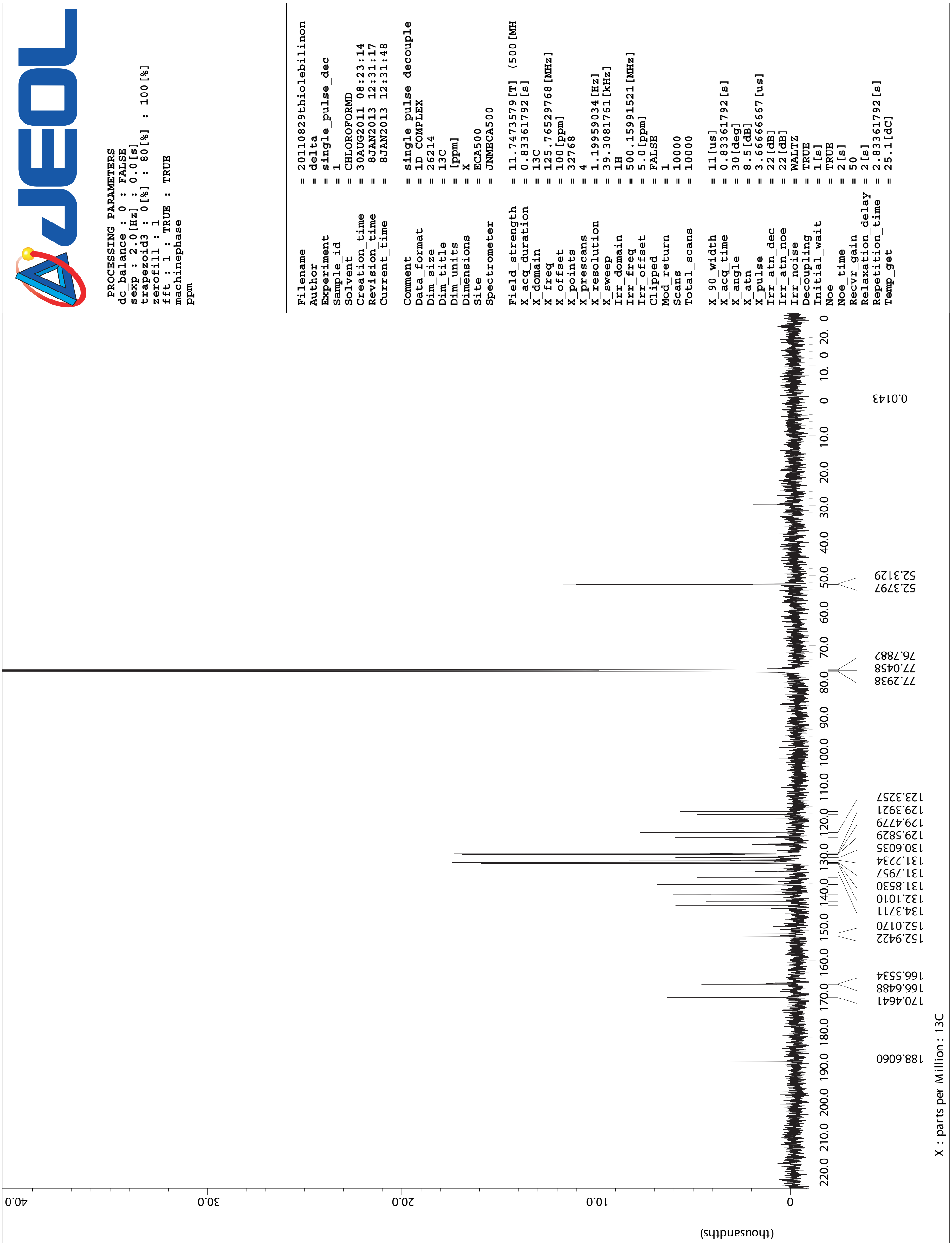

Figure S15. ^{13}C NMR of **8**.

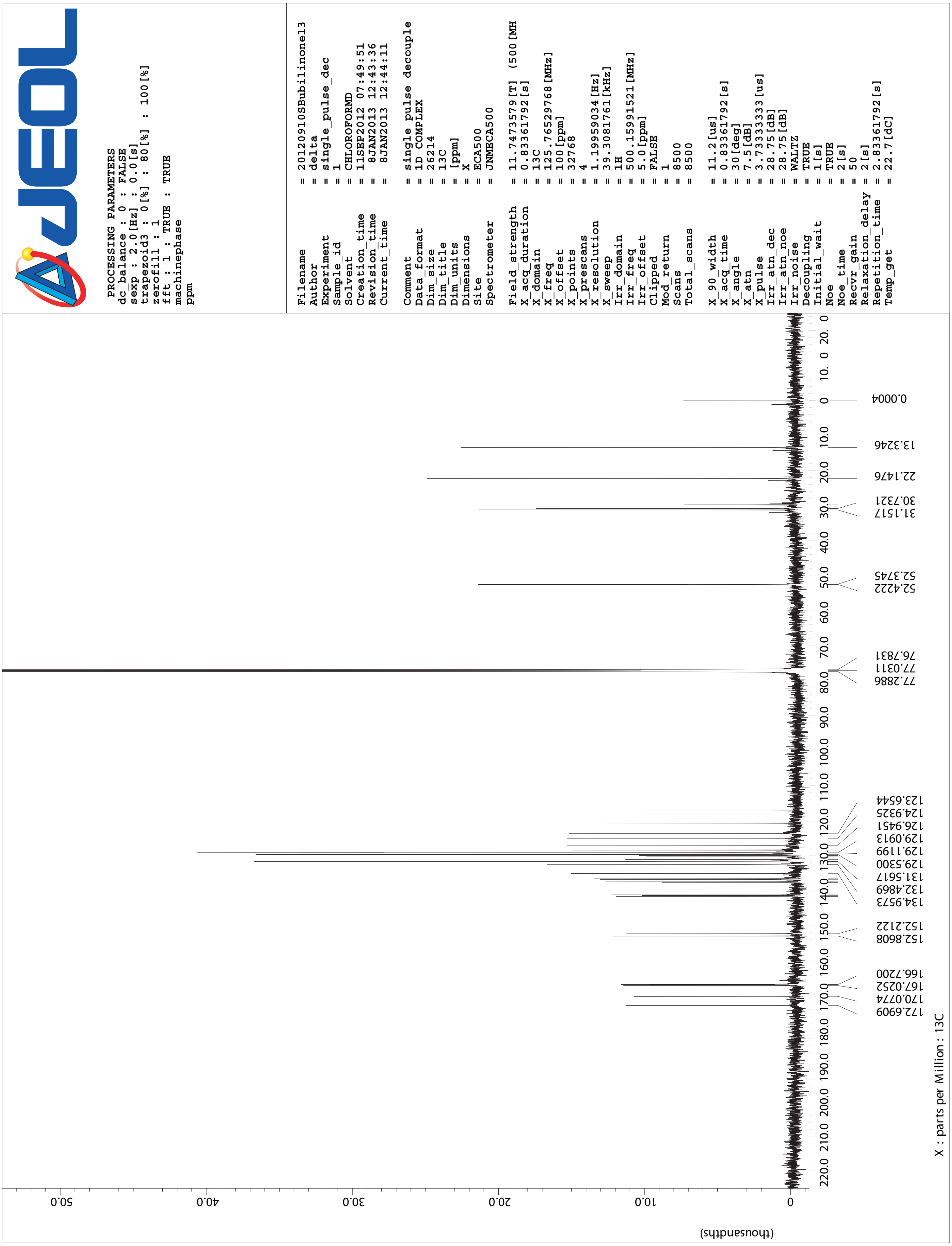

Figure S16. ^{13}C NMR of **9**.

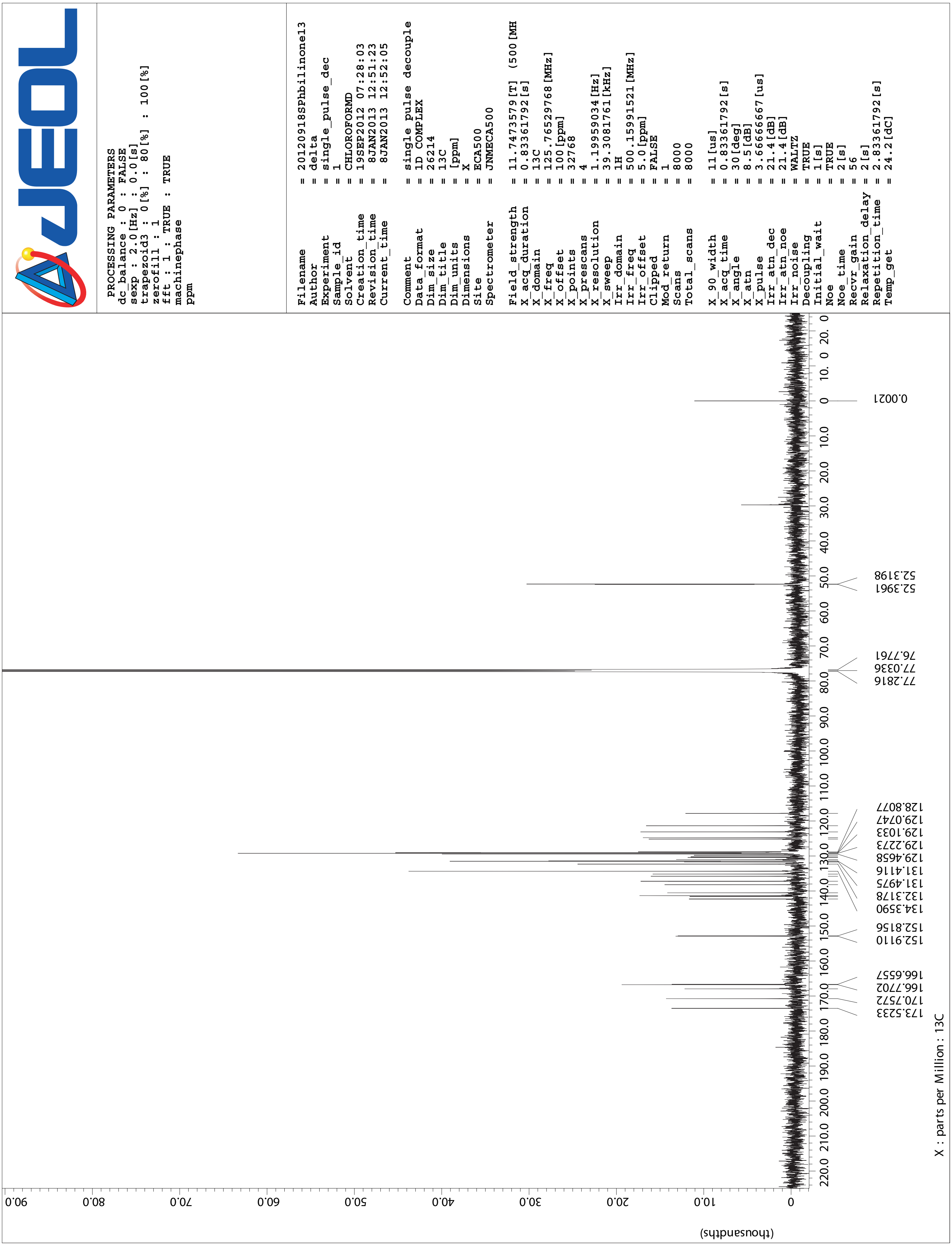

Figure S17. ^{13}C NMR of **10**.

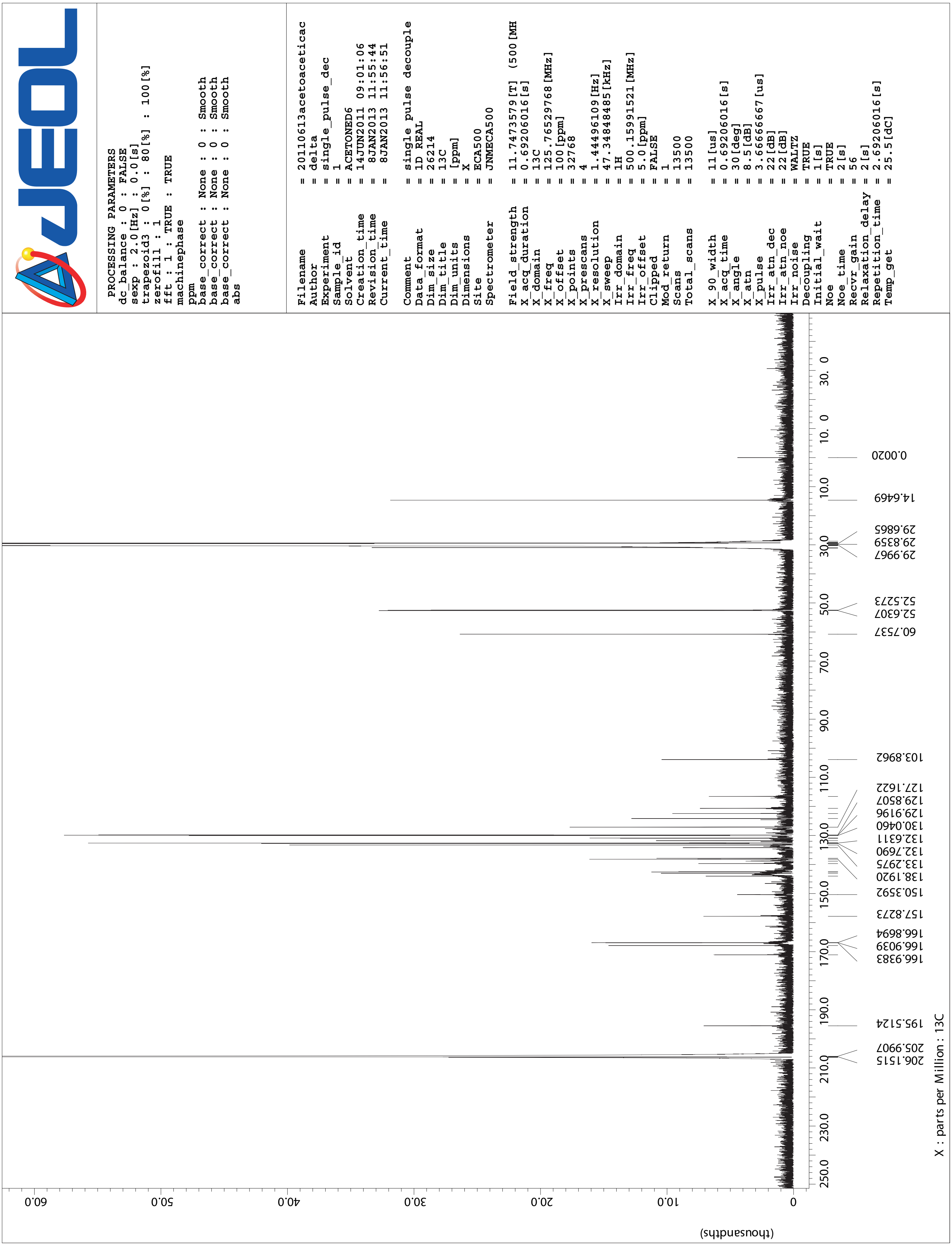

Figure S18. ^{13}C NMR of **11**.

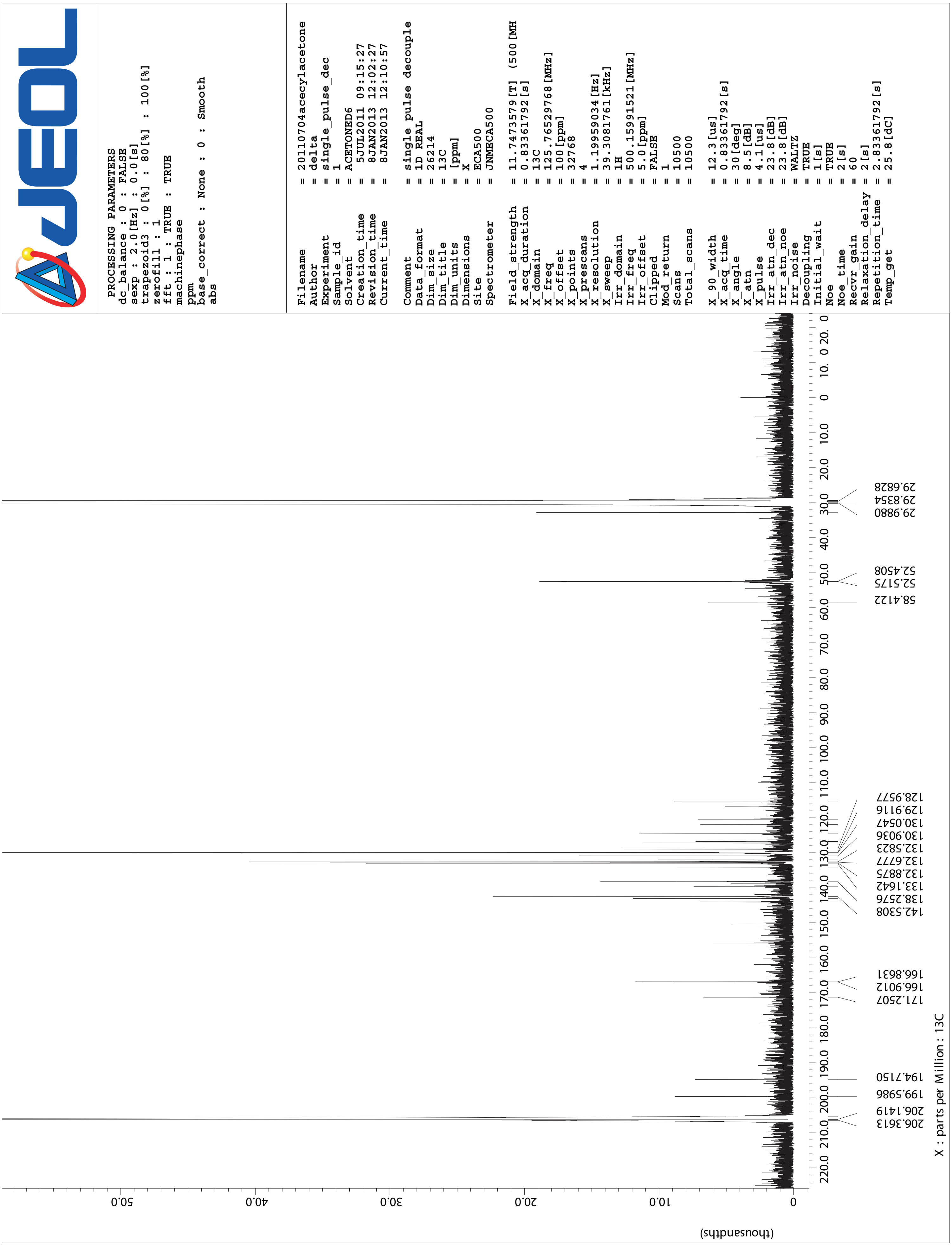

Figure S19. ^{13}C NMR of **12**.

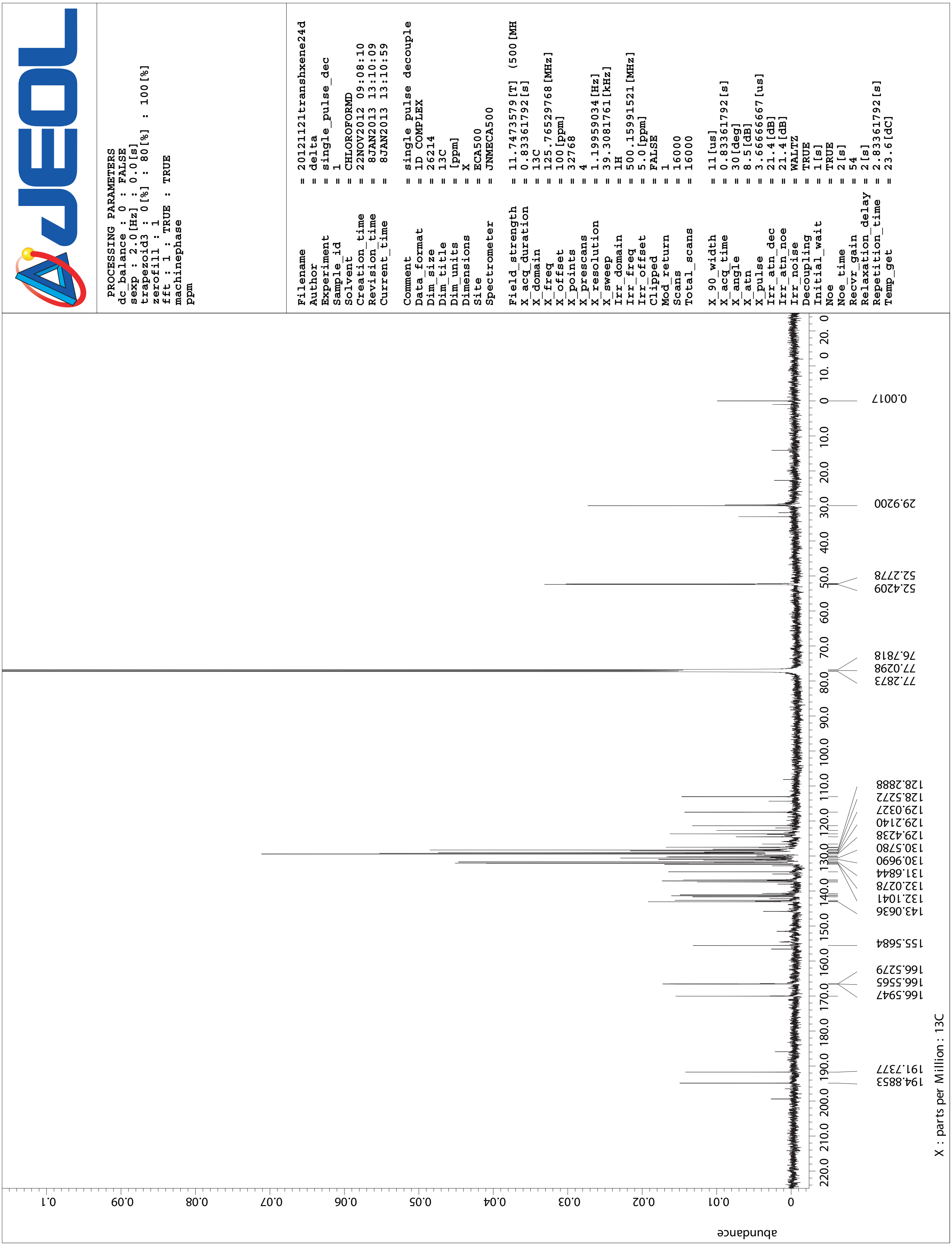

Figure S20. ^{13}C NMR of **13**.

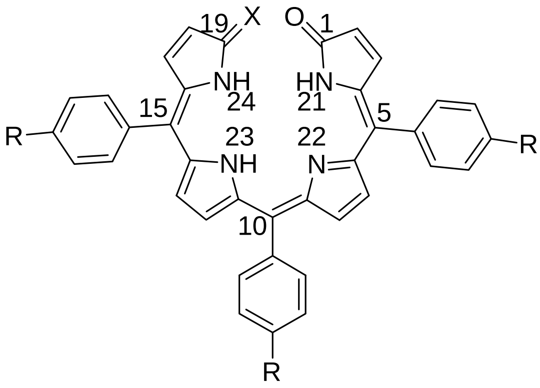

1: R = COOMe, X = O
8: R = COOMe, X = S

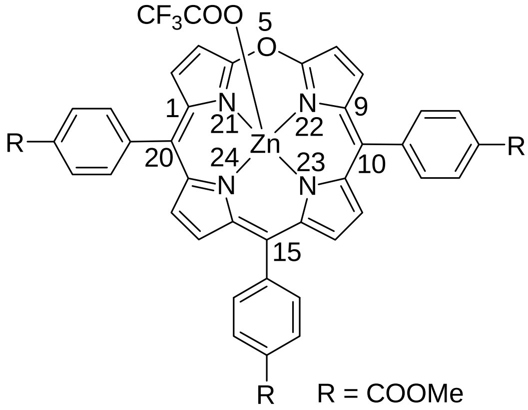

R = COOMe

2

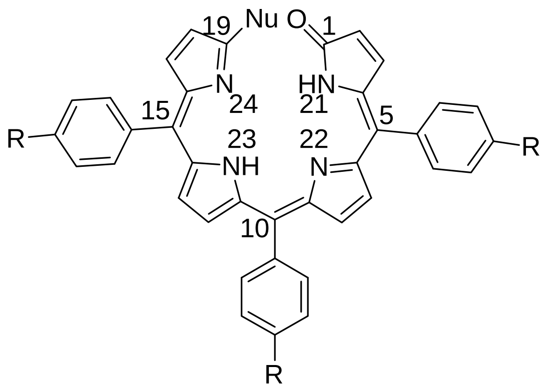

3: R = COOMe, Nu = OMe
4: R = COOMe, Nu = OPh
5: R = COOMe, Nu = NH_2
6: R = COOMe, Nu = NHBu
7: R = COOMe, Nu = NHPh
9: R = COOMe, Nu = SBu
10: R = COOMe, Nu = SPh

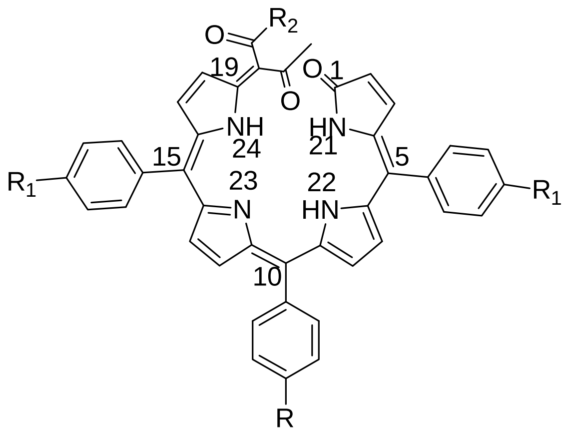

11: R_1 = COOMe, R_2 = OEt
12: R_1 = COOMe, R_2 = Me
13: R_1 = COOMe, R_2 = CH=CHPh

Scheme S1. Numbering scheme of **1-13**.

Table S1. Crystallographic data for **3**.

formula	$C_{47}H_{40}N_4O_8$	V, Å^3	1996.62(8)
formula wt.	788.83	Z	2
color and habit	blue plate	T, K	123(2)
crystal system	triclinic	d_{calcd}, mg cm^{-3}	1.312
space group	P-1	radiation, (λ Å)	Cu K_α (1.54187)
a, Å	7.6123(2)	μ, mm^{-1}	0.739
b, Å	12.0814(3)	range of transmission factors	0.6655 to 0.9640
c, Å	22.5696(5)	$R_1{}^a$	0.0560
α deg	83.4051(13)	$wR_2{}^b$	0.1482
β, deg	83.9689(12)	GOF	1.093
γ, deg	76.2855(12)		

a $R_1 = \sum||F_o|-|F_c||/\sum|F_o|$. b $wR_2 = [\sum[w(F_o{}^2-F_c{}^2)^2]/ \sum[w(F_o{}^2)^2]]^{1/2}$

Table S2. Selected bond distances (Å) of **3**.

O(1)-C(1)	1.222(3)	C(5)-C(6)	1.462(3)
O(2)-C(19)	1.327(3)	C(6)-C(7)	1.442(3)
C(1)-N(1)	1.384(3)	C(7)-C(8)	1.349(3)
C(4)-N(1)	1.385(3)	C(8)-C(9)	1.446(3)
C(6)-N(2)	1.336(3)	C(9)-C(10)	1.391(3)
C(9)-N(2)	1.392(3)	C(10)-C(11)	1.425(3)
C(11)-N(3)	1.370(3)	C(11)-C(12)	1.412(3)
C(14)-N(3)	1.357(3)	C(12)-C(13)	1.371(3)
C(16)-N(4)	1.419(3)	C(13)-C(14)	1.408(3)
C(19)-N(4)	1.304(3)	C(14)-C(15)	1.447(3)
C(1)-C(2)	1.471(3)	C(15)-C(16)	1.373(3)
C(2)-C(3)	1.337(3)	C(16)-C(17)	1.462(3)
C(3)-C(4)	1.457(3)	C(17)-C(18)	1.340(3)
C(4)-C(5)	1.370(3)	C(18)-C(19)	1.456(3)

Table S3. Selected bond angles (degree) of **3**.

O(1)-C(1)-N(1)	125.0(2)	C(10)-C(9)-N(2)	122.5(2)	C(15)-C(16)-C(17)	128.4(2)
O(1)-C(1)-C(2)	130.1(2)	C(10)-C(9)-C(8)	128.7(2)	N(4)-C(16)-C(17)	109.00(18)
N(1)-C(1)-C(2)	104.9(2)	N(2)-C(9)-C(8)	108.69(19)	C(18)-C(17)-C(16)	106.8(2)
C(3)-C(2)-C(1)	108.8(2)	C(9)-C(10)-C(11)	123.4(2)	C(17)-C(18)-C(19)	105.8(2)
C(2)-C(3)-C(4)	109.3(2)	N(3)-C(11)-C(12)	105.76(19)	N(4)-C(19)-O(2)	125.1(2)
C(5)-C(4)-N(1)	125.2(2)	N(3)-C(11)-C(10)	124.2(2)	N(4)-C(19)-C(18)	113.6(2)
C(5)-C(4)-C(3)	129.5(2)	C(12)-C(11)-C(10)	129.9(2)	O(2)-C(19)-C(18)	121.3(2)
N(1)-C(4)-C(3)	105.2(2)	C(13)-C(12)-C(11)	108.4(2)	C(1)-N(1)-C(4)	111.8(2)
C(4)-C(5)-C(6)	121.4(2)	C(12)-C(13)-C(14)	108.0(2)	C(6)-N(2)-C(9)	106.65(18)
N(2)-C(6)-C(7)	110.9(2)	N(3)-C(14)-C(13)	106.6(2)	C(14)-N(3)-C(11)	111.3(2)
N(2)-C(6)-C(5)	121.5(2)	N(3)-C(14)-C(15)	122.7(2)	C(19)-N(4)-C(16)	104.78(19)
C(7)-C(6)-C(5)	127.5(2)	C(13)-C(14)-C(15)	130.7(2)	C(19)-O(2)-C(20)	116.60(19)
C(8)-C(7)-C(6)	106.7(2)	C(16)-C(15)-C(14)	122.4(2)		
C(7)-C(8)-C(9)	107.0(2)	C(15)-C(16)-N(4)	122.6(2)		

Table S4. Selected dihedral angles (degree) of **3**.

O(1)-C(1)-C(2)-C(3)	180.9(2)	C(7)-C(8)-C(9)-C(10)	182.8(7)	C(14)-C(15)-C(16)-C(17)	172.8(5)
C(1)-C(2)-C(3)-C(4)	359.7(3)	C(8)-C(9)-C(10)-C(11)	170.9(6)	C(15)-C(16)-C(17)-C(18)	180.9(1)
C(2)-C(3)-C(4)-C(5)	182.1(1)	C(9)-C(10)-C(11)-C(12)	163.2(8)	C(5)-C(6)-C(37)-C(42)	132.5(4)
C(3)-C(4)-C(5)-C(6)	170.0(6)	C(10)-C(11)-C(12)-C(13)	185.0(5)	C(9)-C(10)-C(29)-C(34)	125.7(3)
C(4)-C(5)-C(6)-C(7)	169.4(6)	C(11)-C(12)-C(13)-C(14)	359.1(8)	C(14)-C(15)-C(21)-C(26)	130.2(9)
C(5)-C(6)-C(7)-C(8)	182.5(2)	C(12)-C(13)-C(14)-C(15)	179.3(9)		
C(6)-C(7)-C(8)-C(9)	359.6(8)	C(13)-C(14)-C(15)-C(16)	166.1(6)		

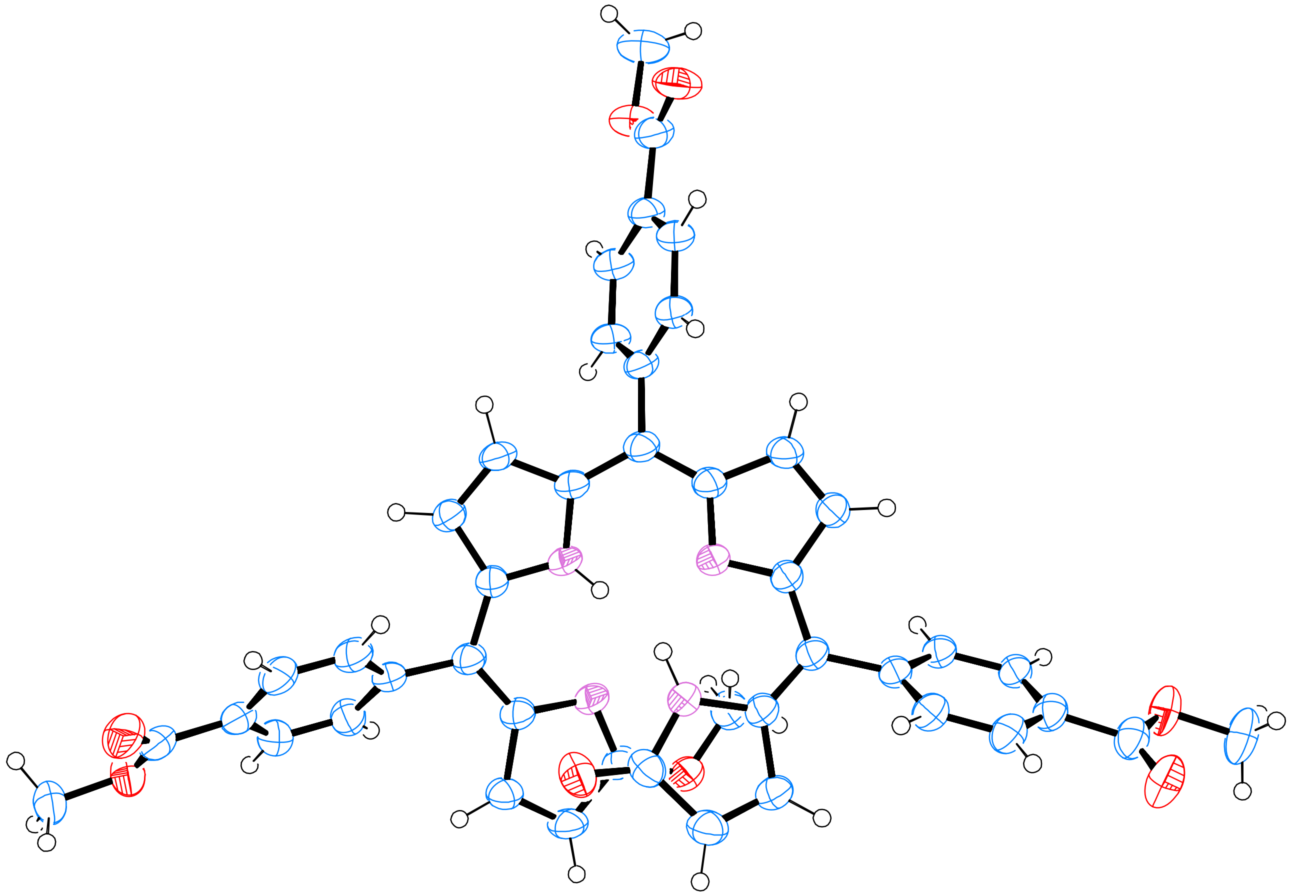

Top view

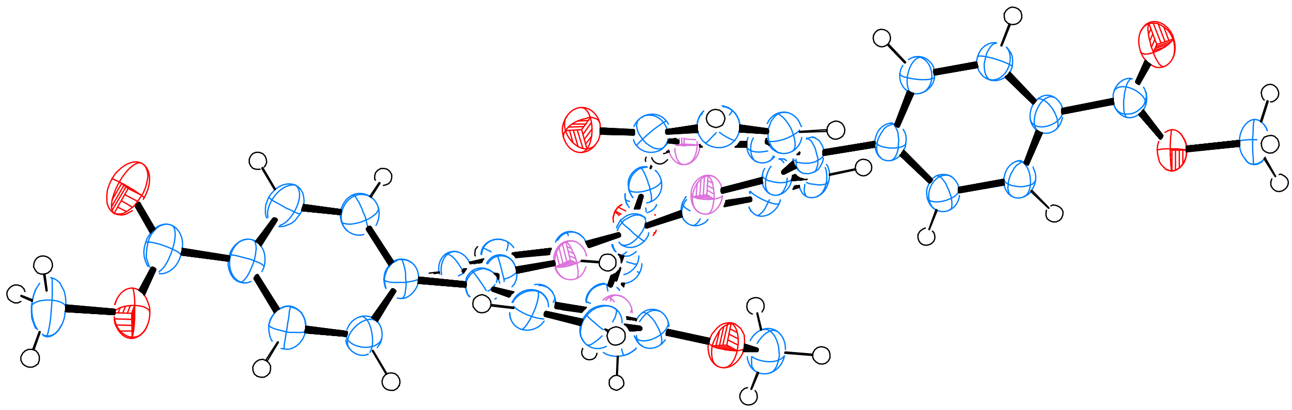

Side view

Figure S21. ORTEP view of **3**.

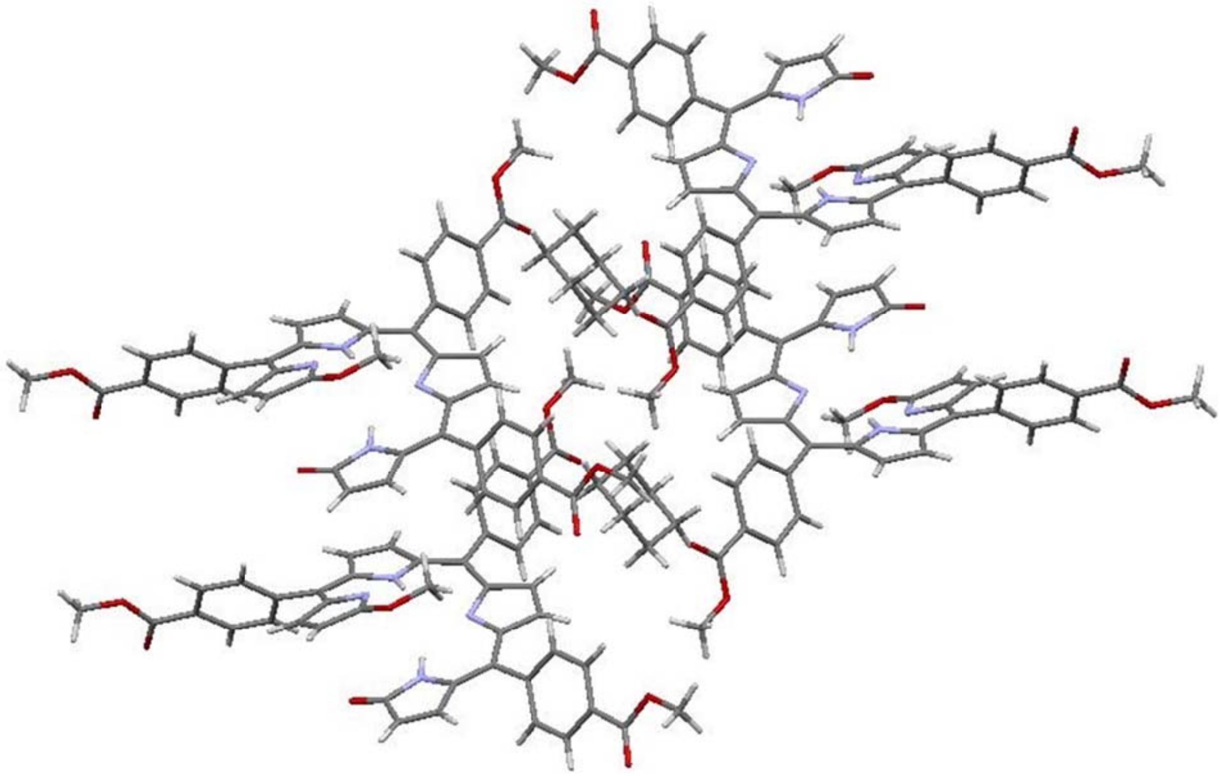

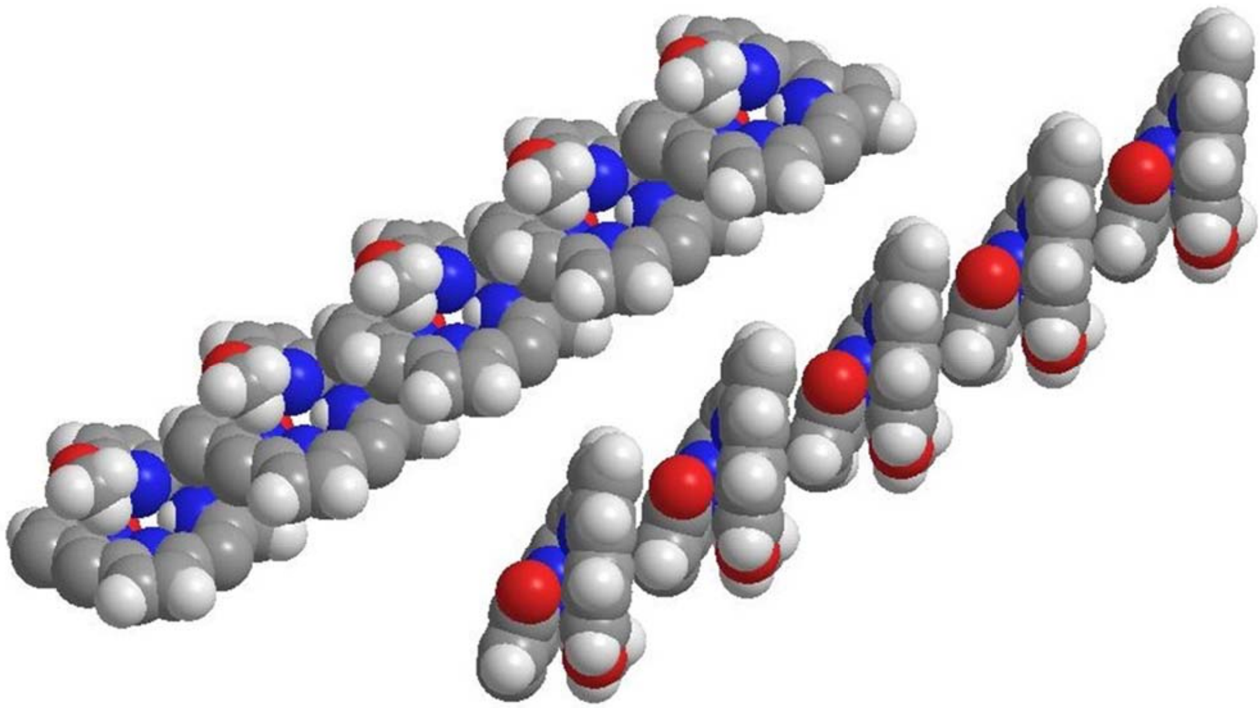

Figure S22. (Top) Cell packing of **3** along the *a*-axis. (Bottom) Structure of spiral column made up of helical molecules. The phenyl groups are omitted for clarity.

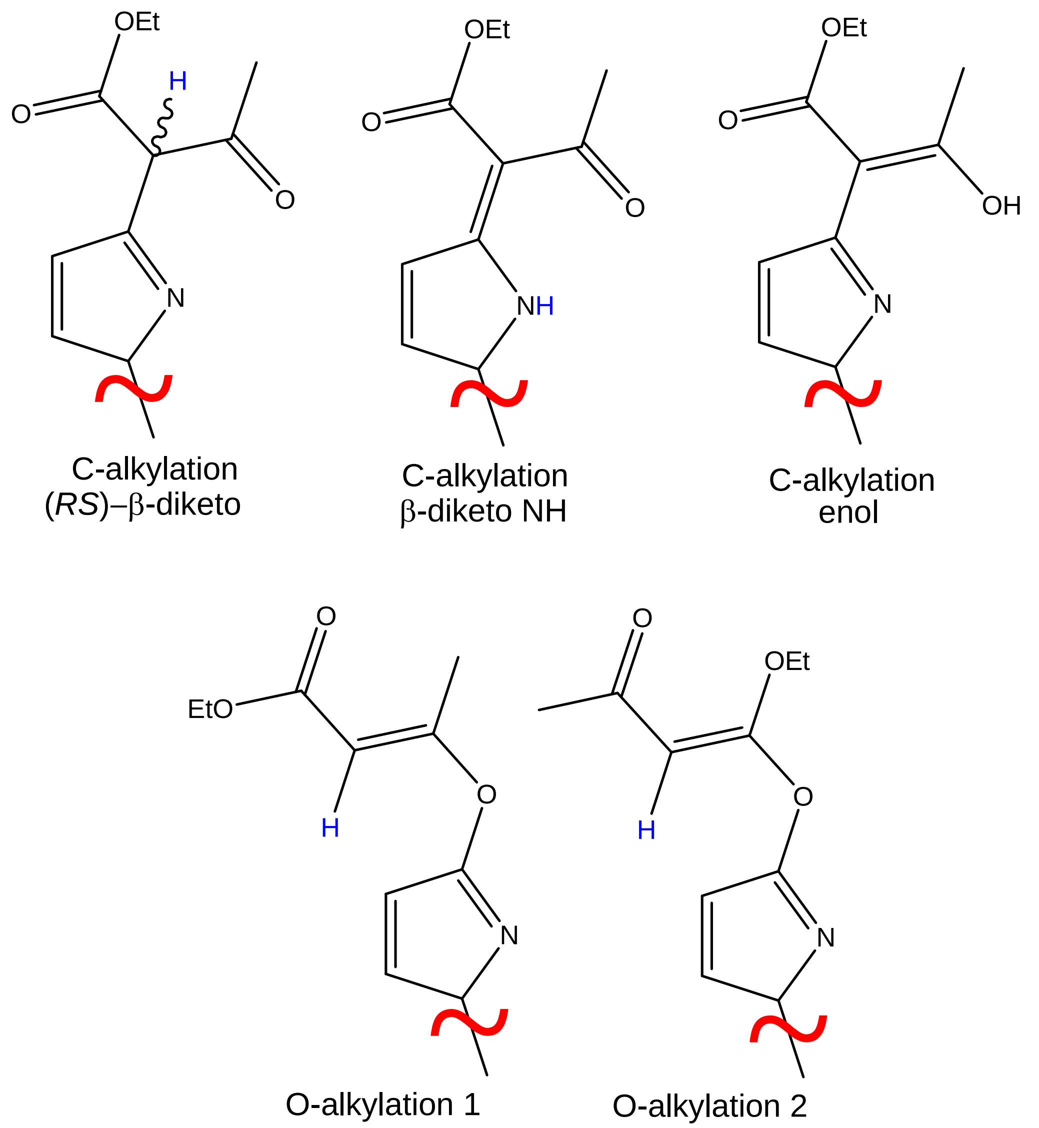

Scheme S2. Tautomeric structures of enolate appended bilinone **11**. Only D-ring is shown.

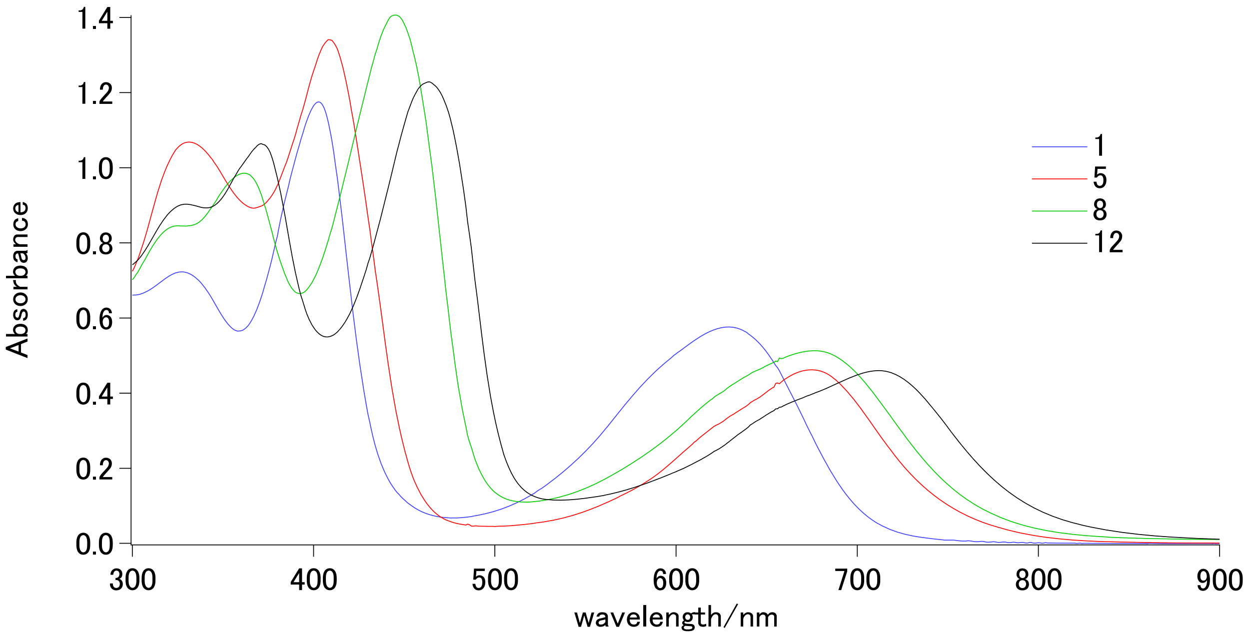

Figure S23. UV-vis spectra of 3 x 10^{-5} M of **1**, **5**, **8** and **12** in $CHCl_3$ at 25 ^{o}C.

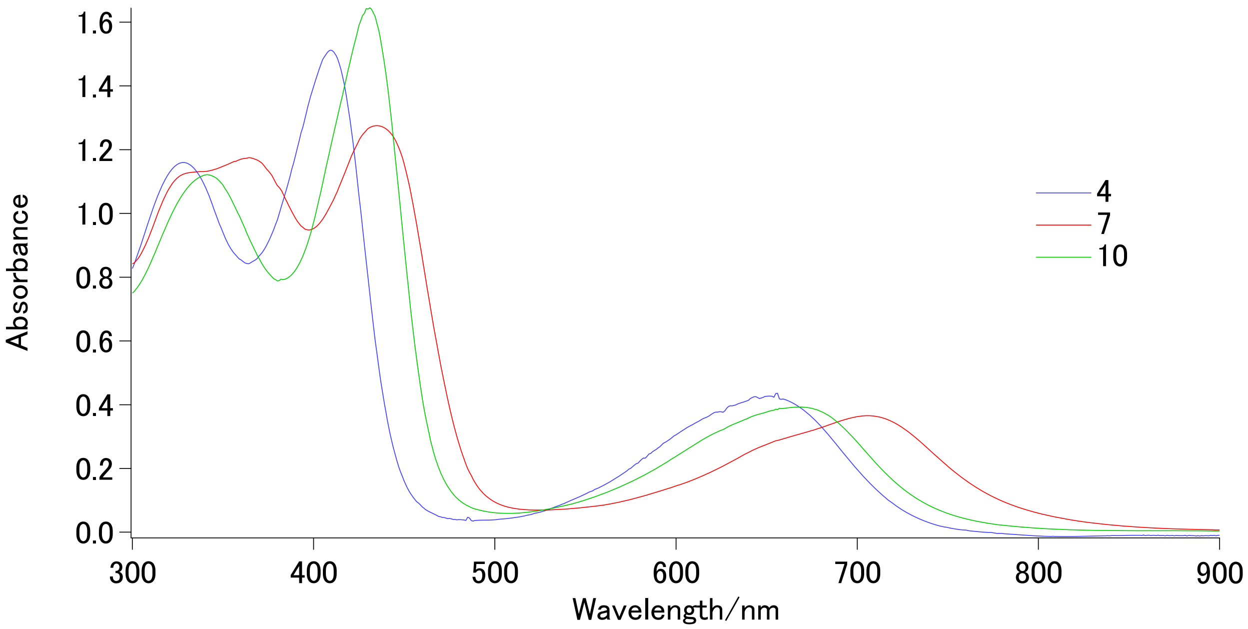

Figure S24. UV-vis spectra of 3 x 10^{-5} M of **4**, **7** and **10** in $CHCl_3$ at 25 ^{o}C.